Electrodiffusion phenomena in neuroscience: a neglected companion

Leonid P. Savtchenko[1], Mu Ming Poo[2] and Dmitri A. Rusakov[1]

Abstract | The emerging technological revolution in genetically encoded molecular sensors and super-resolution imaging provides neuroscientists with a pass to the real-time nano-world. On this small scale, however, classical principles of electrophysiology do not always apply. This is in large part because the nanoscopic heterogeneities in ionic concentrations and the local electric fields associated with individual ions and their movement can no longer be ignored. Here, we review basic principles of molecular electrodiffusion in the cellular environment of organized brain tissue. We argue that accurate interpretation of physiological observations on the nanoscale requires a better understanding of the underlying electrodiffusion phenomena.

Electrodiffusion
Diffusion of charged particles in electric fields.

Electrodynamic events
Time-dependent changes in electric fields or ion distributions.

[1]*UCL Institute of Neurology, University College London, Queen Square, London WC1N 3BG, UK.*
[2]*Institute of Neuroscience, CAS Center for Excellence in Brain Science and Intelligence Technology, State Key Laboratory in Neuroscience, Chinese Academy of Sciences, 320 Yue Yang Road, Shanghai 200031, China.*

Correspondence to D.A.R.
d.rusakov@ucl.ac.uk

doi:10.1038/nrn.2017.101
Published online 19 Sep 2017

Over the past decade, a large section of experimental neuroscience has been cruising steadily towards the nanoscale. From single-molecule tracking in live cells[1] to nano-resolution patch-clamp electrophysiology[2] to voltage-sensitive dye imaging in sub-micron cellular compartments[3], the empirical focus on minuscule physiological events in the brain has continuously been sharpening. In the meantime, the fine cellular microenvironment in which such events unfold has been gradually revealed through the advent of super-resolution imaging methods concentrating on the subcellular architectonics of the live brain[4].

It thus appears that we are approaching a new frontier in our understanding of neuronal structure and function. The rapid advance into the nano-world of neuronal signalling is set, however, to face a theoretical challenge: accurate interpretation of experimental observations. As the key brain functions rely on the electrical activity of nerve cells, translating electrophysiological data into physiological principles has been at the centre stage of neuroscience. In most cases, this gnostic process has relied on the classical theory of electrolytes, adapted to the environment of excitable cells many decades ago.

This long-established theory addresses ion fluxes and electric fields at both sides of the cell plasma membrane[5]. Fully consistent with the early experiments in the isolated giant axon of the squid, its main assumptions have been that the space occupied by the electrolyte on either side of the membrane is much larger than the submembrane diffusion layers and that there is no external source of an electric field. However, both assumptions could be largely invalid in organized brain tissue, which is densely packed with electrically active neurons. Indeed, brain cells *in situ* are constantly exposed to three main sources of electric fields.

The first source consists of the macroscopic, time-varying extracellular fields generated by an average net electric current flow as a result of the spontaneous or behaviour-related (evoked) activity of neuronal assemblies. These macroscopic currents, which are routinely detected by extracellular electrodes as local field potentials, have been a long-rehearsed subject of computational neuroscience because they could provide essential clues to the underlying neuronal activity (for a recent review, see REF. 6). The present Review will therefore touch upon their physiological effects on cells rather than dealing with their mechanistic description. The second source of electric fields is the non-uniform distribution of ion channels and pumps in the neuronal membrane, which can produce a net sub-membrane current, steady in the resting state and transient during spiking[7–9]. The ensuing local voltage gradients could alter the distribution of signalling molecules and thus influence signal propagation in the local circuitry. Third, in the synaptic cleft microenvironment, receptor-channel currents produce focal perimembrane electric fields directed towards or away from the synapse, both extracellularly and in the cytoplasm. The latter could modify the distribution of synaptic components in a synaptic type-dependent manner[10,11].

Because of the relatively small volume of the tissue fraction that is occupied by the extracellular space, the magnitude of extracellular electric fields can be quite substantial. Theoretical estimates[12–14] suggest that they are comparable to the externally applied fields that induce documented lateral electrodiffusion of membrane proteins (such as transmitter receptors) in cultured cells[15,16]. Thus, the classical concept of ion movements referring to a large, electroneutral medium surrounding nerve cells may produce a biased interpretation of electrodynamic events in nanoscopic cellular compartments, such as synaptic clefts or spine necks[17–19].

Our understanding of the nanoscale electrophysiology thus may require more adequate insights into small-scale observations, necessitating theories that would account for the sub-membrane phenomena neglected by the traditional approach (BOX 1). In fact, there has been a rapidly growing body of theoretical and experimental studies, albeit mainly outside neuroscience, dealing with the electrolyte dynamics in conditions that are compatible with the brain cell microenvironment[20–22]. The present Review aims to explain and illustrate some of these re-emerging concepts and their potential implications for nanoscale neurophysiology. We also endeavour to dispel some common misconceptions regarding the nature of the membrane potential while trying not to dwell too much on the well-established electrophysiological postulates, which the reader can find in numerous textbooks (for example, see REFS 23,24). The present Review is by no means intended as an exhaustive guide on electrodiffusion phenomena in nervous tissue, but rather an attempt to discuss theories that are relevant to the electrophysiological phenomena occurring on a small scale, inside and outside cells in the brain.

Basics of electrolytes

Brain extracellular fluid is considered to be a strong electrolyte; that is, an aqueous solution of (fully) dissociated ionic compounds. In resting conditions (no net ion flow), the electrolyte is assumed to be an electrically neutral medium, with zero total charge per unit volume

$$\sum_i z_i C_i = 0 \qquad (1)$$

where the sum is over all *i*th ion species, each having concentration C_i and valence z_i. Electroneutrality is a central principle of the classical electrolyte theory upon which the key electrophysiological derivations have been based. An important and long-established assumption here is

Box 1 | **Nanoscale neurophysiology: classical theories and where they may stumble**

- Inside narrow spaces, local currents can rapidly change ion concentrations. This perturbs electrolyte electroneutrality, rendering the medium conductance — and, hence, the local potential — non-uniform.
- The brain extracellular space often has a smaller cross section and therefore higher local impedance than does the intracellular lumen. In such cases, the membrane potential dynamics will depend mainly on the extracellular medium, in contrast to the classical view.
- Inside narrow extracellular gaps, local fields could be strong enough to prompt lateral movement of charged molecules, as well as an electro-osmotic flow of counter-ions, in and near the plasma membrane.
- Membrane receptors and channels sense electric fields in the nanoscopic proximity of the membrane, whereas patch electrodes report transmembrane potential in the bulk. The relationship between the two measures depends on the composition and surface charge distribution of the membrane.
- Classical theories based on the quasi-static approximation of Maxwell's equations assume no magnetic fields or uncompensated charges, which could be invalid on the nanoscale.
- Molecular electrodiffusion in the synaptic cleft with a receptor current directed towards the centre provides an example of nanoscale neurophysiology. In this case, the Nernst–Planck equation in rotational symmetry gives

$$\frac{\partial C}{\partial t} = D\left(\frac{1}{r}\frac{\partial}{\partial r}\left(r\frac{\partial C}{\partial r}\right) + \frac{zF}{RT}\frac{1}{r}\frac{\partial}{\partial r}rCE\right) \qquad (8)$$

where r is the radial coordinate, $C(r,t)$ is the ion concentration, D is the diffusivity, z is the valence, F is Faraday's constant, R is the gas constant, T is the temperature, and $E(r,t)$ is the electric field. In the steady state (concentrations and currents remain unchanged over the measurement period), $E(r)$ can be expressed in terms of the medium resistivity R, the cleft height h and the current I:

$$E(r) = \frac{dV}{dr} = -\frac{IR_c}{2\pi h r} \qquad (9)$$

Combining (8) and (9) gives

$$\frac{\partial C}{\partial t} = D\left(\frac{\partial^2 C}{\partial r^2} + \frac{1}{r}\frac{\partial C}{\partial r}\left(1 - \frac{zF}{RT}\frac{IR_c}{2\pi h}\right)\right) \qquad (10)$$

where

$$I = 2\pi\int_0^{r_a}(V(r) - V_c)g(r)\,r\,dr \qquad (11)$$

$g(r)$ is the membrane conductance (synaptic current), r_a is the active zone (postsynaptic density) radius and V_c is the conductance reverse potential.

This approach assumes that C shows negligible stochastic fluctuations, which applies to large numbers of molecules. When the numbers are small, the effects of stochastic fluctuations in C could be considerable. Such cases should be addressed through Monte Carlo (single-particle tracking) simulations rather than analytical tools[47,93].

that the spatiotemporal scale of this theoretical application should be greater than that defined by the two following parameters. One is the Debye length L_D (1–2 nm range),

$$L_D = \sqrt{\frac{RT\,\varepsilon_s\,\varepsilon_0}{2F^2C}} \quad (2)$$

where $R = 8.31\ \mathrm{J\,K^{-1}\,mol^{-1}}$ is the gas constant, $F = 96485.3\ \mathrm{C\,mol^{-1}}$ the Faraday constant, ε_s the relative permittivity or dielectric constant of a solvent, $\varepsilon_0 = 8.854 \times 10^{-12}\ \mathrm{F\,m^{-1}}$ the permittivity of free space, and concentration C is defined by

$$C = \sum_i C_i z_i^2 \quad (3)$$

where C_i is the concentration of the ith ion species, and z_i is valence. The other parameter is the Debye time t_D (nanosecond range),

$$t_D = L_D{}^2 D^{-1} \quad (4)$$

where D is the ion diffusion coefficient in the electrolyte[25]. The Debye time refers to the Brownian motion in a free medium without external fields. On the scale smaller than the Debye length, spontaneous Brownian motion of individual molecules incessantly breaks medium electroneutrality[26]. Differential ion mobility or the presence of diffusion obstacles and non-electrostatic interactions between ions and cell walls could exacerbate such effects[22]. Such perturbations are thought to normally arise and dissipate with a time constant shorter than the Debye time.

Importantly, in the bulk of freely moving ions, any spontaneous local accumulation of electrical charge should quickly dissipate because of the rapid (electro-) diffusion of the oppositely charged ions, thus restoring electroneutrality. Therefore, on a macroscopic scale, over the time intervals exceeding t_D, a physiological electrolyte is thought to be electrically neutral. This, however, may change when the theoretical assumptions underlying the electroneutrality principle are no longer valid. The sections below will discuss where and how electroneutrality could be violated and what consequences this may have for our interpretation of empirical observations.

Extracellular medium

Macroscopic electric current. The most straightforward case of electroneutrality violation is a net electric current flowing through the region of interest. A current source (usually located on cell membranes) implies a non-zero current density $j(r)$ across the medium (with coordinates r) (BOX 2). This current gives rise to electric field $E(r)$ present throughout the volume, with its strength depending on local medium conductivity G (BOX 2; Equation 12). Thus, at any time point during the active current phase, one could find a voltage drop between two points in the medium, implying no electroneutrality. In such cases, a complete set of classical Nernst–Planck equations needs to be employed, which in many cases leads to robust quantitative estimates[27].

These theories traditionally work with the classical expression in which the conductivity G depends simply on the steady-state ion concentrations (BOX 2; Equation 13). The formula is a good approximation in the bulk of brain tissue, where a typical electric current alters the steady-state extracellular ion concentration by less than a few per cent. However, this approach should be used with caution when applied to nanoscopic volumes, in which modest ion fluxes could alter ion concentrations many-fold and the current density could be spatially heterogeneous[13,19]. In such cases, G will also depend on local electric field strength E (BOX 2; Equation 14), thus deviating considerably from the classical approach.

Extracellular space heterogeneity. The electrical conductance of the brain extracellular space (volume conductor) directly affects electrogenic events in nerve or glial cells[28,29]. The unit conductance of artificial cerebrospinal fluid at 36–37 °C is ~59 Ω·cm, as reported earlier[14]. However, the actual extracellular conductivity is considerably lower, largely as a result of three contributing factors, as follows. First, the extracellular space in the brain occupies only ~20% of the tissue volume (that is, tissue porosity α~0.2)[30,31], which reduces the ion diffusion coefficient and, hence, the effective conductor cross section accordingly. Second, this space comprises tortuous narrow tunnels and clefts surrounding various cellular obstacles[32,33], with an average macroscopic tortuosity — that is, an effective increase in the diffusion path compared with a free medium — ranging from $\lambda = 1.4$ to $\lambda = 1.6$ (reviewed in REF. 31). Third, even on the nanoscale (no cellular obstacles), ion movement could be decelerated by 30–50% in the extracellular space compared with a free medium[34], probably because of microscopic steric hindrance (fixed or mobile molecular obstacles to diffusion) and viscous interactions[35]. An additional influence may come from the extracellular matrix, which may straightforwardly hinder diffusion[31] or electrostatically interact with ions[36].

The anisotropy and spatial heterogeneity of the extracellular space can lead to non-uniform electric conductivity G and, hence, the emergence of local voltage gradients, which adds to the complexity of establishing the exact values of electric fields throughout the tissue volume (BOX 2; Equation 15; BOX 2; see the figure, parts a,b)[37]. This complication probably affects the interpretation of local field potentials[38] and transmembrane potential recordings for experimentally inaccessible areas, such as dendritic spine necks[19], synaptic clefts[14] or nanoscopic astroglial protrusions[39]. The medium impedance within these narrow spaces could be considerably higher than that of the bulk tissue as a result of the reduced ion concentration and the increased frequency of ion collisions with microscopic obstacles[40]. An accurate theoretical treatment of the extracellular electrodynamics on the nanoscale is still being developed; the classical volume conductor model with the line source approximation[41], a detailed Poisson–Nernst–Planck electrodiffusion theory[7] and the electroneutral approach[8] provide quantitative insights but appear to diverge when dealing with the immediate membrane proximity. Although beyond the scope of this

Debye length
(L_D). A scale over which the free charges, and therefore the electric field, are screened by an electrolytic solution.

Debye time
(t_D). The average time required for an ion to travel one Debye length.

Extracellular matrix
A loose mesh, or possibly a hydrogel-like structure, composed of fibrous proteins and polysaccharides that fill the interstitial space in the brain (and other tissues).

Anisotropic media
Media that display different properties in different directions, whereas the properties of isotropic media or fields do not depend on direction.

Second-rank conductivity tensor
A measure of conductivity is a 3 × 3 array (matrix) of values that characterize medium electrical conductivity in the x, y and z directions.

Dielectric media
Media that cannot conduct electric current.

Inner Helmholtz layer
A layer that is formed in the sub-membrane space by cations that are attracted to the negatively charged cell membrane surface.

Electrical double layer
(EDL). A layer that is formed by free-diffusing electrolyte ions in the nanoscopic proximity of a charged surface, with the immediately adjacent layer of opposite-sign ions followed by a more diffuse layer of same-sign ions.

Review, there has also been a concerted effort to understand extracellular electricity in the context of electroencephalography (EEG) analyses and macroscopic field recordings[6,42].

Vicinity of cell membranes

Membrane surface charges and the adjacent ion layers. It is common knowledge that an electric charge generates an electric field that interacts with other charges. There is a fundamental difference between the spatial distributions of electric fields generated in dielectric media (for example, dry air) and those generated in electrolytes. In the former case, the electrostatic electric field follows the basic principle of Coulomb's law and, in theory, extends into infinity (FIG. 1a). In electroneutral electrolyte solutions, however, this field extends only within a short distance comparable to the Debye length. Beyond the Debye length, mobile ions compensate for the influence of the field, making the bulk of the electrolyte electroneutral (FIG. 1a). The underlying phenomena can be understood by exploring the nanoscopic region near the phospholipid cell membrane surface, which is negatively charged (FIG. 1b). The charged surface prompts the formation of the inner Helmholtz layer of cations, which is immediately adjacent to the membrane, and another layer (more loosely formed because of a greater effect of Brownian movement), thus forming an electrical double layer (EDL), roughly within the Debye length from the surface (FIG. 1b). The main features of this double layer depend on ion concentrations, the membrane charge density and the thickness of the membrane. The Gouy–Chapman theory proposed a century ago was the first successful attempt to quantify this type of EDL at a phase boundary[26]. Its main assumptions (BOX 3) enabled robust, if only approximate, theoretical derivations for the electric field near cell membranes. The theory has since been adapted and modified for various sub-membrane scenarios, and its limitations have been explored in detail[43,44].

More recently, it has emerged that multicompartmental, Monte Carlo or hybrid (combined-type) computer models of sub-membrane ion layers could provide a more direct and arguably more accurate tool to understand ion behaviours in the sub-membrane electrolyte. In a typical hybrid model, Monte Carlo computations (which track the Brownian motion of individual particles) are carried out within the small volume of interest. At the same time, the flows of particles crossing the volume boundary are continuously recalculated into the flux, field and other parameters representing boundary conditions for the compartmental or analytical model adopted for the large (or infinite) surrounding volume[45–48].

Computer simulations that account for differential mobility and hydration radii of ions have suggested, for instance, that a bulk Ca^{2+} concentration of a few millimolar corresponds to levels of up to 50 mM near the cell membrane[49], in qualitative agreement with earlier analytical estimates[50]. Detailed electrochemical simulations have proposed that in physiological solutions (akin to the cerebrospinal fluid), the medium electroneutrality could be violated within ~2 nm from the ion-permeable membrane, and over a time interval of up to 40 µs (REF. 51). Intriguingly, the latter timescale is

Box 2 | Basic relationships between electric field, current and conductance in electrolytes

The field strength $\boldsymbol{E}(r)$ arising from an external current

$$\boldsymbol{E}(r) = \frac{\boldsymbol{j}(r)}{G} \quad (12)$$

where $\boldsymbol{j}$ is the current density, and r is the spatial coordinate. The conductivity $G(r)$ for strong electrolytes is given by

$$G = \frac{F^2}{RT}\sum_{n=1}^{N} D_n z_n^2 C_n \quad (13)$$

where z_n, C_n and D_n are the valence, concentration and diffusivity, respectively, of the nth ion species, and T is the temperature. Expression (13) represents a traditional interpretation of electrophysiological recordings: it assumes overall electroneutrality and therefore uniform conductivity G, which depends on the bulk ion concentration only. However, when electric fields perturb local ion concentrations C_n, the electroneutrality can be violated. In such cases, G (see the figure, part **a**; green shade scale) will relate inversely to $\boldsymbol{E}(r)$ (see the figure, part **a**; black arrows illustrate its direction and relative strength), thus giving constant $\boldsymbol{j}$ (grey arrows). Thus, G could depend on the spatial coordinate r:

$$G(r,E) = \frac{F^2}{RT}\sum_{n=1}^{N} D_n z_n^2 C_n(r,E) \quad (14)$$

In this context, fluctuations in the local concentration of any ion should trigger concentration changes in all other ions as the system drives to electroneutrality. In addition, the classical linear dependence between G and C_n assumes that C_n are sufficiently low to neglect direct molecular interactions. Increasing C_n and thus inter-ion interactions could disproportionately decrease G[120].

In a general case involving anisotropic media[37,121], field and current vectors $\boldsymbol{E}$ and $\boldsymbol{j}$ are not necessarily collinear (see the figure, part **b**). Their relationship can be described as

$$\boldsymbol{J}_i = \boldsymbol{G}_{ik}\boldsymbol{E}_k \quad (15)$$

where $\boldsymbol{G}_{ik}$ is a second-rank conductivity tensor, which scales and rotates $\boldsymbol{E}$ with respect to $\boldsymbol{j}$. The current in this case will flow along the three-dimensional path of lowest electrical resistance (see the figure, part **b**; grey arrows indicate direction of $\boldsymbol{j}$, which is rotated with respect to the direction of $\boldsymbol{E}$). It is important to note that, according to the essentials of thermodynamics, there cannot be 'residual' ion current that occurs without electric field in electrolyte, as this would violate the principle of increasing entropy[121].

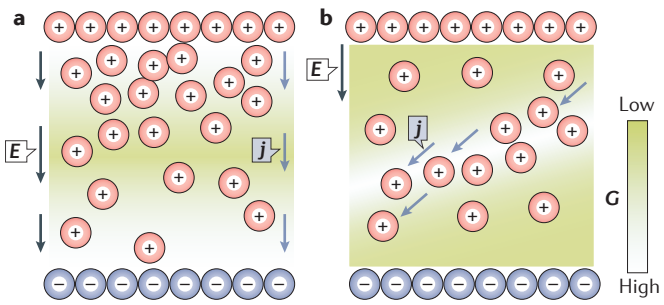

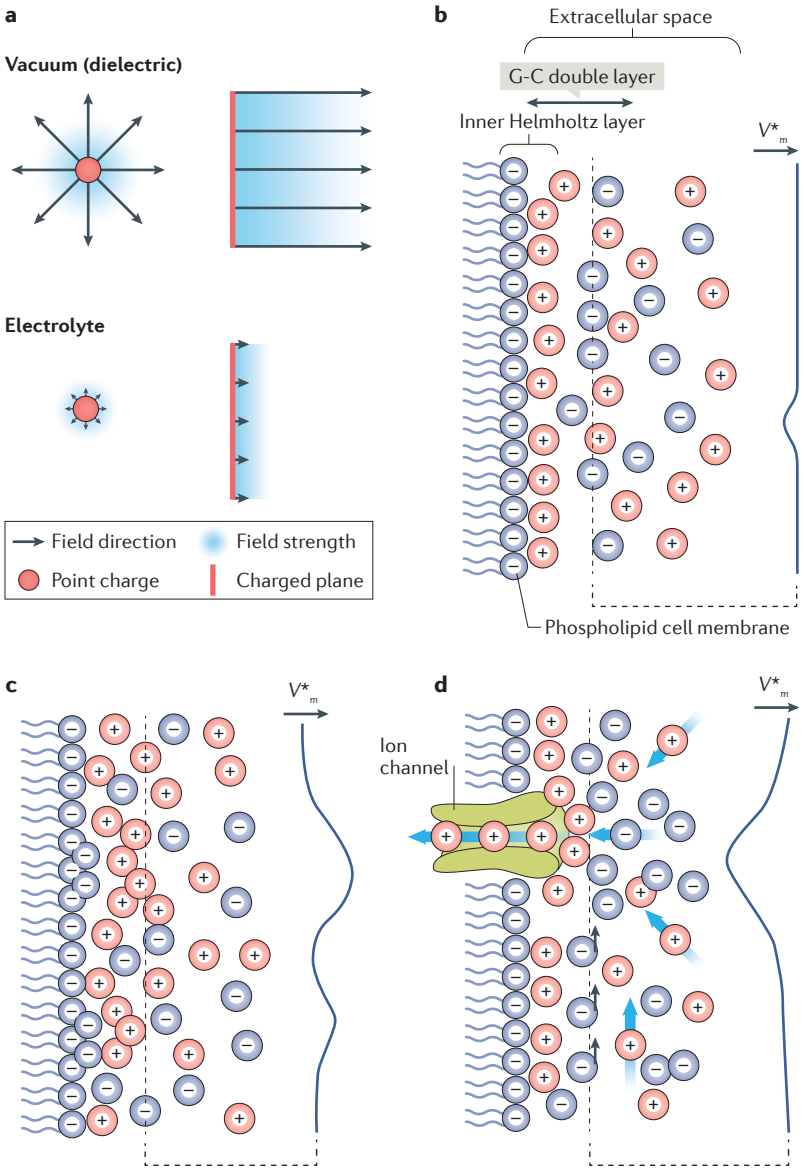

Figure 1 | **Electric charges and their fields in brain tissue: basic principles and two common deviations from common electrophysiological postulates. a** | The schematic depicts electrostatic electric fields generated by a local (point) charge and a charged plane, in either a vacuum (dielectric medium, top) or an electrolyte (bottom). The colour intensity illustrates the field strength. Whereas the field (depicted by arrows) in a vacuum extends into infinity, fields in electrolytes are highly localized. **b** | The panel shows ion distributions and the local voltage profile near a negatively charged phospholipid cell membrane surface; the inner Helmholtz layer (a layer of cations lined up next to the negatively charged membrane) and Gouy–Chapman double layer (G-C; includes the Helmholtz layer and a loose layer of anions adjacent to it) are indicated. V^*_m depicts the voltage profile (arrow indicates voltage scale) at a short distance from the membrane (dotted line, not to scale) from which signalling proteins such as ion channels may sense local electric fields (see below). The V^*_m profile shows a canonical case of a nearly evenly charged membrane. **c** | The schematic depicts heterogeneity in sub-membrane ion distribution and local voltage owing to excessive membrane charges (carried by either phospholipids or membrane proteins). The uneven occurrence of cations (red) and anions (blue) reflects the variable density of local electric fields and hence the heightened variability of the sub-membrane voltage V^*_m compared with that in part **b**. **d** | This panel depicts heterogeneity in sub-membrane ion distribution and local voltage owing to ion channel currents. Blue arrows depict the current direction (an ion channel is shown in green). Black arrows depict drag forces exerted by the cation current flow; these forces tend to drag particles alongside the sub-membrane ion layers.

comparable with the rising phase of the transmembrane current during action potential generation[52]. Because the sub-membrane extracellular medium is likely to remain heterogeneous over such time intervals, the accurate translation of such measurements into membrane potential could be complicated. With the growing availability of large-scale computation resources required for such models, progress in the area is likely to accelerate.

Heterogeneous lateral landscapes of membrane surface charge. Because of the non-uniform cellular trafficking and turnover of membrane proteins and phospholipids (including their random fluctuations), the surface charge could be distributed unevenly. This heterogeneity generates lateral, steady-state electrical fields that perturb the classical ion double layer, leading to an uneven redistribution of electrolyte ions in the plane of the membrane (FIG. 1c). The resulting profile of the sub-membrane voltage becomes correspondingly heterogeneous (FIG. 1c). A full description of this complex system in a steady state involves multiple sources of positive and negative feedback, which can be described, with some degree of accuracy, by a set of nonlinear differential equations[7,9]. We note here that the uneven landscape of sub-membrane charges will not only generate laterally heterogeneous voltage but also directly affect the transmembrane potential, as explained in the sections below.

Local channel-mediated current. In another common scenario, a current flows through individual ion channels, generating lateral ion movement along the membrane (FIG. 1d). Given a sufficiently high ion density in the vicinity of the membrane, this flow can exert viscous drag (that is, pulling along the adjacent liquid layers through friction) involving both charged and neutral particles such as water molecules (FIG. 1d). In a classical Helmholtz–Smoluchowski approximation, just outside the sub-membrane double layer, the electric field E should prompt sub-membrane lateral flow with velocity v, so that

$$v = -\varepsilon_r \varepsilon_0 \zeta E/\eta \quad (5)$$

where ε_0 is the permittivity of free space, ε_r is the dielectric constant of the aqueous phase, ζ is the cell surface potential and η is the viscosity of the extracellular medium. The flow rate drops quasi-exponentially with the distance to the membrane, roughly with the Debye length constant. These basic effects give rise to the lateral forces acting upon membrane proteins and may therefore induce their rearrangement. As explained in the sections below, this phenomenon could contribute to the nanoscopic organization and dynamics of important membrane specializations, such as receptor-protein mobility and clustering in the postsynaptic density.

Membrane potential: measured versus actual

Key assumptions in measuring V_m. Classically, transmembrane potential V_m is determined by the free electrical charges accumulated at the two sides of the cell membrane, in accord with Donnan equilibrium

Gouy–Chapman theory
Classical formulas to describe the formation of diffuse charged layers occurring in the vicinity of a charged surface (membrane) as a result of free diffusion of small ions.

Monte Carlo
Models that rely on computational algorithms that employ random number generation to mimic naturally occurring stochastic events, such as molecular Brownian motion.

Boltzmann distribution
Sometimes called a Gibbs distribution, this is a probability distribution of the stochastically behaving particles being in a certain state.

Poisson–Boltzmann theory
Equations that describe the electrochemical potential of ions in the diffuse layer.

Continuum limit
A theoretical approximation in which, at certain limiting scale, discrete (binned) system elements are considered as a continuous parameter or feature of the system.

Van der Waals interactions
Attractive or repulsive intermolecular forces that are not related to (and are normally weaker than) covalent bonds or electrostatic forces. These interactions may include dipole interaction, hydration or lipophilicity, among others.

V^*_m potential
The local electric field in the membrane proximity that drives voltage sensors of ion channels and other voltage-sensitive membrane proteins.

Liquid junction potential
(LJP). A potential that arises at a non-selective boundary between two electrolytes with different ion concentrations or mobility.

and Goldman–Hodgkin–Katz theory: to calculate V_m, one must address the Nernst–Planck equation and Poisson equation by using the electrolyte composition and membrane permeability, which can be found in textbooks on electrophysiology[23,24]. In healthy neurons, there is an excess of positive charges outside, which results from the different ion composition found inside and outside, from the action of selective ion channels and pumps and from the presence of impermeable ions in the cytoplasm (*ibid*).

It is important to note that the sub-membrane voltage generated through local charge accumulation is what essentially controls the voltage-dependent activity of membrane proteins such as ion channels. Their molecular voltage sensors are driven by electric fields in the nanoscopic proximity of the membrane surface (reviewed in REFS 53,54), illustrated in sections below as sub-membrane V^*_m potential (FIG. 1b–d), rather than being directly dependent on the V_m readout obtained with electrodes away from the membrane. In patch-clamp practice, however, one inevitably refers to a voltage difference V_m between the cell cytoplasm and the bulk of the extracellular medium, as gauged by the current measured in a closed electric circuit (FIG. 2a). The medium around the recording electrodes is routinely assumed to be equipotential and electroneutral, with no electric field present. In fact, the act of recording does violate macroscopic electrolyte electroneutrality, albeit very slightly: this violation is required to generate the ion current providing a voltage readout (FIG. 2a). The case is similar to that of monitoring water pressure in a large vessel in which a small leak should serve the purpose, with no detectable effect on the water level (FIG. 2a).

Non-stationary liquid junction potential. Perhaps the most common empirical factor that could bias macroscopic V_m measurements is the liquid junction potential (LJP)[55]. Upon a contact between two electrolytes with distinct ion compositions or mobility, excess charge emerges at the interface, generating a local electric field (FIG. 2b). In the simplest case of two binary electrolytes with ion concentrations C_1 and C_2, it is given by the Henderson equation

$$\Delta\varphi = \frac{u_+ - u_-}{u_+ + u_-}\frac{RT}{F}\ln\left(\frac{C_2}{C_1}\right) \quad (6)$$

where u_+ and u_- are the ion mobility. The formula assumes electroneutrality (no strong current) inside and outside the electrode. Three LJP types have classically been considered[56]: the same salts at different ion concentrations, different salts at similar ion concentrations and different salts at different ion concentrations. While LJP can be estimated with various online calculators (for example, http://web.med.unsw.edu.au/phbsoft/LJP_Calculator.htm) on the basis of known ion concentrations, recent studies emphasize that the LJP is not in a steady state[27,57]. During the continued dialysis and solution mixing, this interface could expand away from the electrode, with the boundary charge density decreasing and the ion concentrations partly equilibrating (FIG. 2b).

Distortions invisible to patch clamp. As noted above, one of the key factors affecting V^*_m on the nanoscale is the distribution and screening (cancelling out by the nearby opposite charges) of electric charges carried by molecules at or near the cell membrane surface, which contribute to the Gouy–Chapman EDL[58]. If the surface

Box 3 | **Key assumptions of the Gouy–Chapman theory of the electrical double layer**

- Ions in the solution are modelled as point charges, thus neglecting their physical dimensions and arising singularity.
- The solvent is considered a dielectric continuum with dielectric constant ε.
- The average concentration of ions at a given point reflects the average of the electrostatic potential at that location, in accord with the Boltzmann distribution, which is a probability function *F(S)* of the stochastically behaving particles being in a certain state *S* in a multi-particle system: $F(S) \sim \exp(-\Psi/kT)$ where Ψ is the state-designated energy, $k = 1.38 \times 10^{-23}$ m^2 kg s^{-2} K^{-1} is the Boltzmann constant, and *T* is the temperature in Kelvin.

Approximations routinely employed in derivations exploring sub-membrane ion layers (largely based on the Poisson–Boltzmann theory) include the following:

- the membrane is treated in a continuum limit as an interface with a contiguous surface charge distribution, with no point or discontinuous features such as ion channels;
- the electric potential and the ion charge densities are described by continuous variables;
- non-electrostatic interactions, such as van der Waals interactions, are neglected; and
- membrane boundaries or curvature are not considered.

Common approximations and assumptions in theories dealing with macroscopic extracellular electric fields include the following:

- the extracellular space is homogeneous and isotropic, with a constant unit conductance;
- ions move in the extracellular space without boundary effects, friction or steric hindrance;
- in baseline conditions, the principle of electroneutrality is held throughout the medium so that free particle diffusion is assumed;
- the effects arising from water molecule movement are neglected and;
- the condition of electroneutrality is maintained at infinity in the equations.

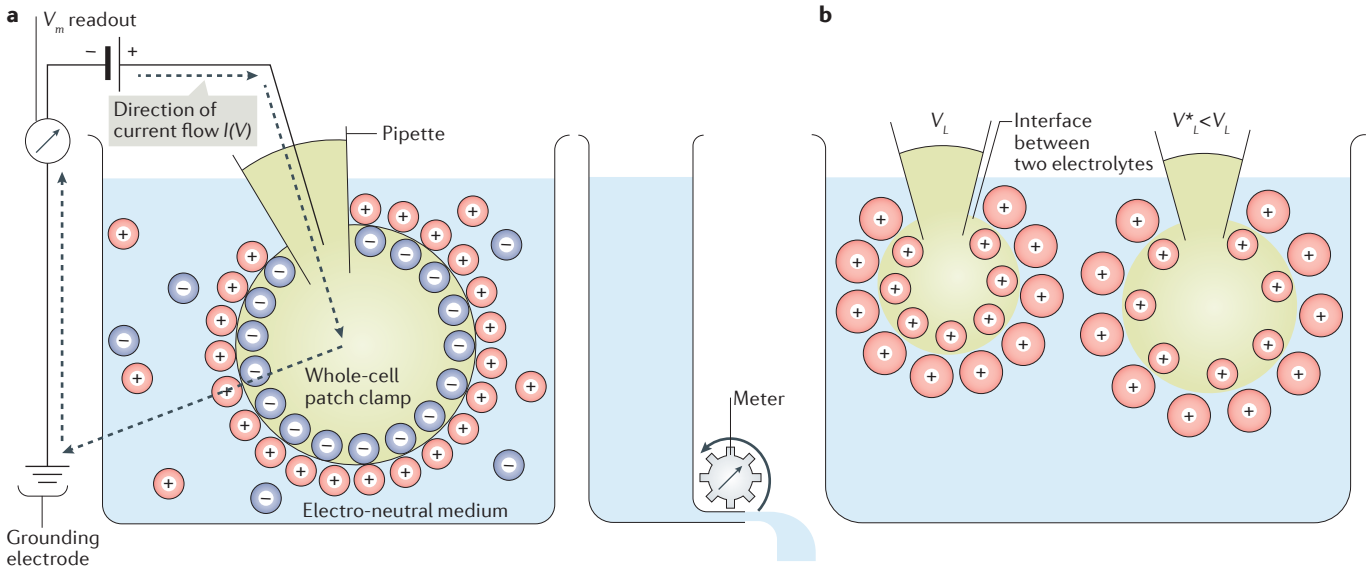

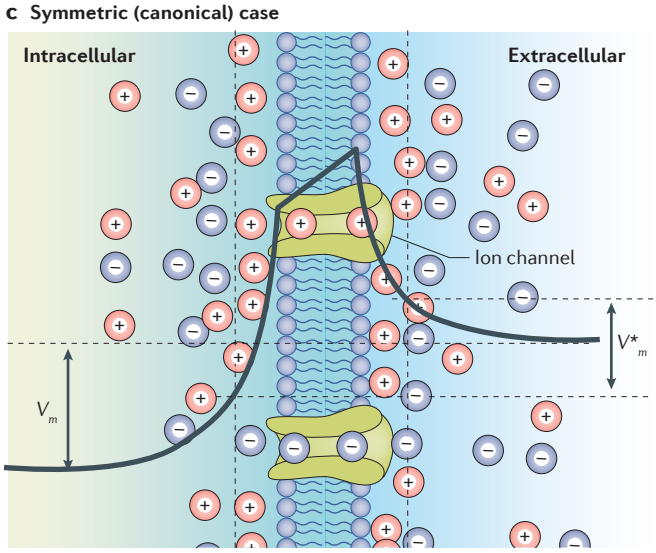

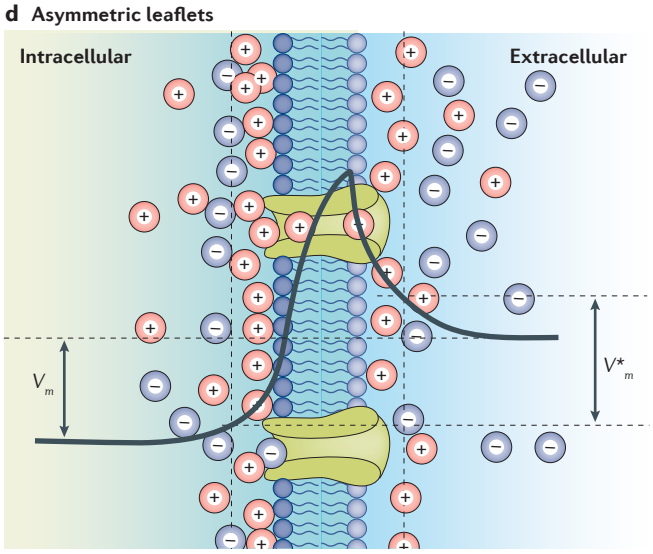

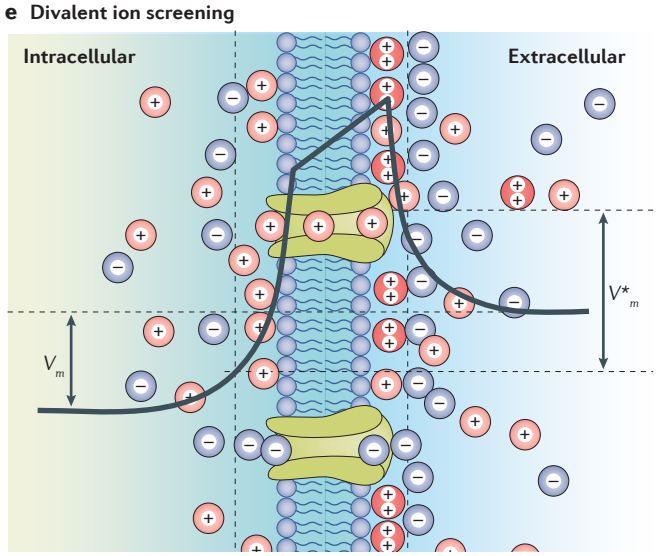

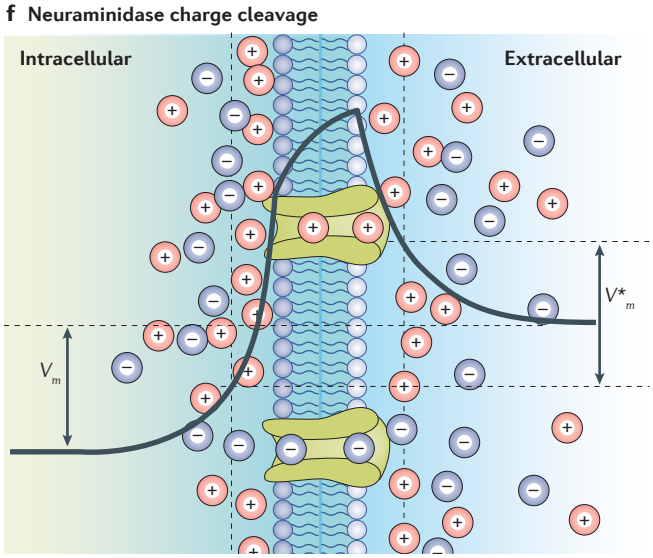

◀ Figure 2 | **Patch-clamp measurements of membrane potential: first principles.** **a** | Simplified diagram of a standard patch-clamp configuration; membrane potential is depicted by the excess positive charge outside the cell. Taking a measurement of current *I*(*V*) involves a breakdown, albeit almost negligible, of the medium electroneutrality. Inset, a water pressure analogy of V_m measurements: the rate of a small leak can be used to evaluate water pressure (height of potential) in a large volume, without affecting the water level. **b** | Diagram illustrating non-stationary liquid junction potential (V_L) at the interface of the pipette solution (green) and bath solution (blue; no cells present). When the two solutions have distinct ion compositions and/or ion mobility, this gives rise to a *trans*-interface electric field (shown by the accumulation of two different ion types at the solution interface). During the dialysis, the boundary can expand and/or dissipate, thus reducing the liquid junction potential to a new value $V_L^* < V_L$. **c–f** | Common distortions of transmembrane potential that are invisible in a patch-clamp configuration. A schematic depicts the cell membrane bilayer and sub-membrane ion layers; *V* (thick grey line), the 'true' voltage profile across the membrane; V_m, transmembrane voltage measured in patch-clamp configuration, away from the membrane; vertical dotted lines, the approximate sub-membrane locality that primarily affects the channel voltage sensor; V^*_m, transmembrane voltage sensed by ion channels at that locality (as in FIG. 1b–d). **c** | Symmetric (canonical) case. Because sub-membrane electric fields quickly dissipate away from the membrane, the measured membrane potential V_m is likely to be somewhat larger than the sub-membrane V^*_m sensed by the receptors and channels. **d** | Asymmetric leaflets. The effect of the two asymmetrically charged membrane (bilayer) leaflets; the inside leaflet is shown to be more negatively charged, shifting the *V* profile (grey line) accordingly. This increases the V^*_m compared with the canonical case, with little effect on the V_m measured by the patch pipette, the latter thus underestimating V^*_m. **e** | Divalent ion screening. The effect of the divalent ion (red circles) screening of the membrane charge; this screening extends the characteristic intramembrane *V* profile (grey line) outside the membrane leaflet, again increasing V^*_m with no effect on V_m. **f** | Neuraminidase charge cleavage. The effect of metabolic activity (the negative charge cleavage with neuraminidase; white circles depict loss of negative charge); again, this situation increases the local transmembrane voltage drop V^*_m with little effect on the pipette readout V_m.

charge landscapes carried by the inner and outer membrane leaflets are roughly mirrored, the net field generated by EDLs across the membrane does not distort the sub-membrane local V^*_m or pipette-measured macroscopic V_m (FIG. 2c). Although this scenario is thought to be relatively common, an asymmetric distribution of neutral lipid molecules, in particular sphingomyelin or cholesterol, in one of the two membrane leaflets can modify the surface charge and thus the local V^*_m potential[59,60] (FIG. 2d). The latter, in turn, would shift accordingly the activation curve of voltage-sensitive membrane proteins that occur nearby.

Divalent ion screening. An even more prominent influence on V^*_m may come from the variable ratios of divalent and monovalent cations in the solution. Divalent cations (for example, Ca^{2+} and Mg^{2+}) have a greater charge with a smaller effective radius and therefore provide more efficient screening of negative surface charges (FIG. 2e). When the concentration of divalent ions changes inside or outside the cell, the overall charge-screening efficiency may also change and thus alter the voltage drop across the membrane. This change could have a substantial effect on voltage-gated ion channels that sense local V^*_m, and thus on cell excitability[61], without necessarily affecting patch-clamp measurements of V_m. Such phenomena could be activity-dependent: for instance, neuronal discharges could transiently lower local extracellular [Ca^{2+}] (from its normal level of 1.5–2.0 mM) as a result of Ca^{2+} entry[62] or indirect consequences of Na^+ entry[63] into neurons. This in turn would have a disproportionately large effect on sub-membrane [Ca^{2+}] (which could reach a 50 mM range because of the favourable conditions for Ca^{2+} accumulation near the negatively charged membrane, compared with Na^+ or K^+)[49]. Indeed, early calculations[49,50] suggested that 1 mM divalent ion added to 100 mM electrolyte would shift the membrane potential by ~26 mV because of the screening effect. With these considerations in mind, classical studies of ion channels have routinely documented voltage-dependent channel properties over a range of divalent ion concentrations[64,65]. It would seem important for the electrophysiological observations of today to account for such phenomena.

Biochemical and metabolic modification of surface charges. Finally, a potentially crucial contributor to V^*_m could be the biochemical or metabolic alteration of the membrane surface charge density through interaction with other molecules. One important example is the changes in the membrane charge landscape through sialylation by neuraminidase (an enzyme that cleaves sialic acids); this reaction is a common part of molecular signalling cascades in the brain. Sialylation can cause a large depolarizing shift in the activation curve of voltage-gated sodium channels, also altering the spiking threshold of the neuron, without any change in the patch-clamp-recorded membrane voltage V_m in hippocampal pyramidal neurons[66]. This is because the removal of negative surface charges increases (hyperpolarizes) V^*_m, with little effect on V_m (FIG. 2f), thus making it more difficult for the external depolarizing current to activate sodium channels. Modification of voltage-gated channels through sialylation could be a common phenomenon across various types of excitable cells[67], and it might potentially explain the role of extracellular matrix proteins in regulating cell excitability and synaptic plasticity[68–70]. The aggregation of membrane proteins may also result in local changes in the surface charge density, which in turn would affect protein function. In a key demonstration of such phenomena, the burst duration of acetylcholine (ACh) receptor–channel kinetics was significantly prolonged in the muscle cell membrane when ACh receptors were induced to form a stable aggregate in the membrane after an exposure to a physiologically relevant extracellular electric field (10^2–10^3 V/m) (REF. 71).

Intracellular space

General notes. It has long been acknowledged that in thin dendrites and dendritic spines of nerve cells, the dynamics of the ion concentration and the membrane potential follow the Nernst–Planck equation, rather than the cable equation[72]. This is because in small volumes, the ion concentration cannot be assumed constant, which is a key prerequisite of the cable equation. However, this valid correction has not been widely used, most likely owing to the complex numerical calculations involved and the difficulty of measuring local membrane potential. Subsequently, there had been several attempts

Sialylation
A biochemical reaction in which sialic acid (an N- or O-substituted derivative of neuraminic acid) groups are introduced into oligosaccharides and carbohydrates as the terminal monosaccharide.

to improve the solution accuracy for small spaces by introducing fractional Nernst–Planck equations combined with the corresponding fractional cable equations, to model ion electrodiffusion in nerve cells[73,74]. Although the cable equation still provides a well-trodden path to study cell membrane electrodynamics, efforts are being made at adopting the Nernst–Planck equations more widely to model electrogenic processes in neurons and glia more accurately[75,76].

Cell-impermeable anions and perturbation of electroneutrality. The cell cytoplasm hosts a variety of cell-impermeable anions (CIAs) — proteins, hydrogen phosphate groups, sulfates and other organic macromolecules — that remain negatively charged at intracellular pH[77]. These macromolecules are surrounded by cytoplasm cations, thus perturbing the cytoplasm electroneutrality, at least on the nanoscale (FIG. 3a). Such perturbations could form local ion layers and, correspondingly, electric fields that could affect local molecular signalling mechanisms.

Interestingly, the effective concentrations of the negative charges carried by CIAs could reportedly reach concentrations as high as 100–200 mM (REF. 78). It has recently been suggested that the actively regulated intracellular redistribution of such protein-associated CIAs effectively controls the intracellular chloride concentration, thus impacting GABAergic transmission[79]. This idea was based on the simple postulate that, to maintain the net sums of charges inside and outside the cell, the redistribution of CIAs in the cytoplasm could effectively displace other anions, mostly chloride. This interpretation was later challenged by providing alternative, physiologically relevant explanations of the original experimental observations[80–82], but whether it is, in principle, biophysically plausible has remained uncertain.

Assuming that individual CIAs are evenly distributed in the aqueous cytoplasm, 100–200 mM corresponds to an average volume density n ~0.1 nm^{-3}, and thus an average nearest-neighbour distance of ~$0.62n^{-1/3}$ = 1.34 nm. This distance is comparable with the Debye length for 100–200 mM strong electrolytes at physiological temperatures. In this case, the CIAs could, in theory, displace chloride ions, as there will be limited space left for forming screening layers and maintaining a free electroneutral (chloride-containing) medium in between individual CIAs. However, this simplified calculation assumes that individual CIA charges and small

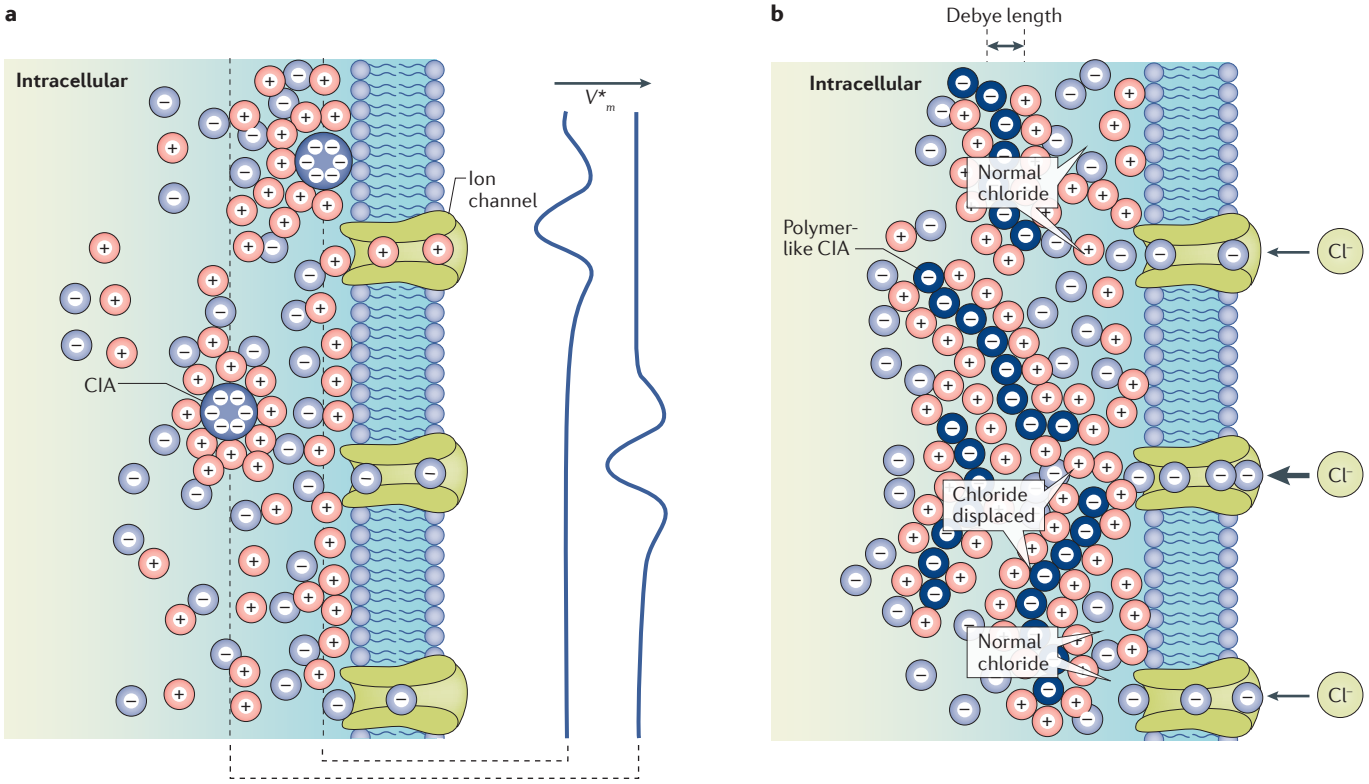

Figure 3 | **The effect of membrane-impermeable intracellular anions on transmembrane ion exchange. a** | A schematic depicting large cell-impermeable anions (CIAs; blue circles) surrounded by a layer of cations; the local excess of positive charge and adjacent anions means that the local lateral voltage profile (V^*_m) is not uniform but has the corresponding local deviations. **b** | A schematic depicting a large concentration of polymer-like CIAs (blue chains) surrounded by cations; such CIAs can displace Cl^- ions within a Debye length, with normal Cl^- concentration occurring elsewhere. An increase in cations and Cl^- displacement in the immediate vicinity of membrane channels (but not away from them) could locally increase the driving force for Cl^- entry. The high charge density of CIAs, while providing a high average charge concentration value, corresponds to a small fraction of the cytosol volume, leaving large areas of unperturbed electroneutrality.

cytosol cations (mainly chloride) form an ideal-gas-type thermodynamic equilibrium, which is probably not the case, as explained below.

Small volume occupied by CIAs should leave enough room for free anions. In fact, detailed biophysical studies of the intracellular milieu indicate that macromolecule-associated CIAs are grouped in polymer-like structures forming an intracellular hydrogel 'matrix' (REFS 83–85) that is intrinsically sensitive to osmolarity and pH[86]. Although featuring a high surface charge density (nominally exceeding 200 mM on the nanoscale), such structures appear to occupy only a small fraction of the cytosol volume[87], thus effectively permitting virtually free diffusion of small molecules in between them[88]. Similar logic applies to the effects of intracellular organelles bearing a surface charge: for instance, in physiological conditions, actin filaments of the cytoskeleton bear the charge at a linear density of ~$4{\cdot}10^3$ *e*/μm (REF. 89). It has recently been estimated[90] that, in such cases, the charge-screening ion layers are formed around the densely accumulated surface charges, while the bulk of intracellular electrolyte remains in an equilibrium with free-diffusing ions such as chloride (FIG. 3b). The 'cloud' of ions surrounding such structures serves as a Debye shield, forming a narrow cable-like arrangement. The prevalence of an electroneutral, mostly equilibrated electrolyte explains the relatively unrestricted diffusion of various signalling molecules in the cytosol.

Therefore, it appears that, unless a local displacement of chloride by CIAs occurs in the immediate intracellular vicinity of chloride channels, the driving force for chloride is unlikely to be influenced by CIAs (FIG. 3b). Nonetheless, the exact features of ionic landscapes inside the neuronal cytoplasm remain incompletely understood[83]. Because slowly moving or immobile proteins or intracellular organelles could thus affect local electroneutrality, the mechanism of intracellular voltage regulation appears complicated, involving multiple timescales.

Narrow extracellular spaces

Neurotransmitter electrodiffusion in the synaptic cleft. The most intense extracellular fields generated endogenously in the nervous system seem to occur near excitatory synapses. Either spontaneous or evoked release of transmitters (glutamate or ACh) could trigger inward membrane currents through the postsynaptic clusters of transmitter receptor channels, with the focal extracellular fields pointing towards the synaptic cleft and the cytoplasmic fields pointing away from the synapses. Thus, it has long been noted that when a synaptic inward current flows through receptor channels in the middle of a narrow synaptic cleft, a considerable lateral voltage drop can form across the cleft[12,91]. In the bulk of the cleft volume (away from the membrane), ion diffusion can be described by classical equations of electrodiffusion (BOX 1). Such focal electric fields may serve three different purposes at the synapse: formation, maintenance and activity-dependent plasticity.

The relatively small ratio of extracellular to cytoplasmic volume (0.1–0.2) dictates that the extracellular electric field must be much stronger than the cytoplasmic field. Estimates based on the synaptic current measurements point to the electric fields peaking in excess of 10^2 V/m, which may exist at the synaptic cleft[92]. In the case of small central synapses equipped with synaptic glutamate receptor channels of the AMPA and NMDA types, detailed Monte Carlo modelling suggests that the sodium current flowing from the outside can give rise to a local field reaching ~10^4 V/m inside the cleft[13,14].

Although this strong field can only slightly perturb local pre-equilibrated concentrations of the prevailing extracellular ions, such as sodium or potassium[47], experiments have indicated that it can accelerate diffusional escape of glutamate molecules (negatively charged at physiological pH) by twofold to threefold following their release and receptor activation[47,93] (FIG. 4a). When glutamate release happens to coincide with the postsynaptic spike (that is, sharp reversal of the current and hence of electric fields), electrodiffusion slows down glutamate escape, thus boosting activation of local high-affinity receptors (FIG. 4a; note that the bulk of high-affinity glutamate uptake occurs further away, outside the cleft). Such electrodiffusion-driven activation of the otherwise 'silent' high-affinity receptors could trigger synaptic plasticity, as shown for perisynaptic metabotropic glutamate receptors at cerebellar synapses[47] (FIG. 4a). In studying such phenomena, a routine assumption has been that external electric fields have no effect on the ligand–receptor binding per se. Although this notion has been supported, at least in part, by detecting no effect of intra-cleft fields on receptor currents activated by electrically neutral GABA[93], the net influence of electric fields on receptor binding requires further studies.

Protein migration in the synaptic cleft under electric fields. It has long been proposed that focal currents generated by the nascent synaptic connections give rise to electric fields that may help to recruit plasma membrane and cytoplasmic components for the establishment of pre- and postsynaptic specializations, in a positive-feedback manner[94]. One could assess the overall effect of transient electrostatic forces on charged membrane proteins by calculating the molecule's velocity v in a viscous membrane medium. As the viscous resistance depends highly supra-linearly on v, the velocity value quickly stabilizes and becomes linearly proportional to the electric field in accord with the classical relationship:

$$v = D\left(\frac{F}{RT}\right) f_e = D\left(\frac{zF}{RT}\right) E \qquad (7)$$

where f_e is electrostatic force, E is electric field, D is the intra-membrane diffusion coefficient, and z is valence. With the E value reaching ~10^4 V/m inside the cleft[14,93], this expression predicts a force of ~10^{-15} N. Given the expected lateral diffusion coefficient for major synaptic receptors (AMPA and NMDA receptors) of ~50 nm^2/ms (5–100 nm^2/ms range[95,96]), v will be in the range of ~50z nm/s. There is a paucity of data shedding light on the net electrostatic charge carried by extracellular compartments of synaptic receptors, let alone the uncertainty about the relationship between such charges

Hydrogel
An intracellular or extracellular network of polymer-like molecules that often carry a high-density surface charge, with a flexible structure sensitive to the bulk pH and osmolarity.

Intracellular organelles
Specialized subunits or multi-molecular complexes that are equipped with a specific function inside a cell.

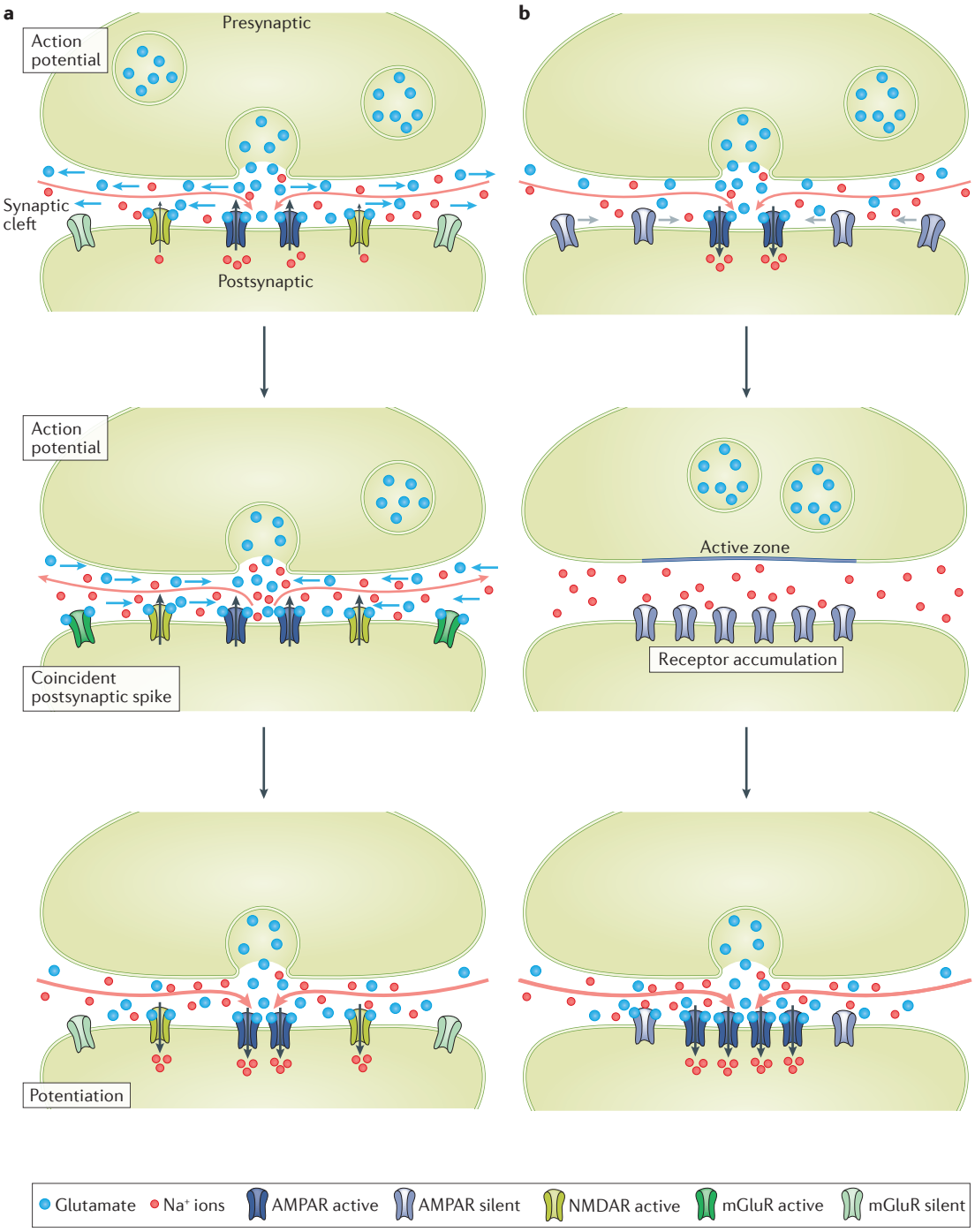

Figure 4 | **Possible physiological implications of electrodiffusion and electro-osmosis in the synaptic cleft.** **a** | An AMPA receptor (AMPAR) current generated shortly after the release of glutamate (*top*, blue dots) gives rise to a strong flux of sodium ions (red dots) towards the cleft centre (red arrows), thus creating an electric field reaching 10^3–10^4 V/m, which accelerates glutamate escape (blue arrows). However, when receptor activation coincides with a postsynaptic action potential (middle panel), the flow of sodium ions (red dots) is directed away from the active AMPA receptor locations (red arrows), thus reversing the field. In the latter case, glutamate is temporarily retained in the cleft; in cerebellar synapses, this retention can boost activation of perisynaptic metabotropic receptors (middle panel), resulting in a potentiated NMDA receptor (NMDAR) response (bottom), which in turn alters signal integration in the circuit[47]. **b** | An AMPA receptor current generated shortly after the release of glutamate (top) is carried by a strong flux of sodium ions towards the cleft centre (red arrows). The centripetal flow of sodium can exert both electrostatic and electro-osmotic drag upon the charged sub-membrane ion layers including receptor protein domains (top, grey arrows). This drag could hypothetically prompt AMPA receptor accumulation at the cleft centre, nearer to the neurotransmitter release site (middle), thus leading to a potentiated synaptic current (bottom). mGluR, metabotropic glutamate receptor.

and the immediate molecular environment. One protein structure study has estimated that NMDA receptors could carry an extracellular positive surface charge in the region of $z = 20–30$ (REF. 97). This would correspond to $\nu = 1–1.5$ nm/ms, predicting that the 100–200 ms inward current (characteristic time for the synaptically activated opening of NMDA receptors) could, in theory, move NMDA receptors towards the peak current source by many tens of nanometres (FIG. 4b). Although the post-synaptic receptor clustering could be triggered by other mechanisms, such as Brownian diffusion with traps[98] or the presence of cooperative membrane surface binding sites[99], the faster timescale provided by electrodiffusion remains an attractive proposition for rapid receptor re-arrangement.

After the synapse matures, turnover of synaptic components (exchange of newly synthesized proteins with the old ones) in the plane of plasmalemma and in the cytoplasm[100,101] may be facilitated by the constant presence of these focal fields generated by spontaneous or evoked transmitter release. Similarly, in the course of use-dependent plasticity, such as long-term synaptic potentiation induced by intense neurotransmitter release[102], electric fields might enhance recruitment of synaptic components such as synaptic receptors via lateral migration[10,103,104] (FIG. 4b).

Other narrow spaces. Similarly to the case of synaptic clefts, the narrow space between cell walls could lead to a high local current density and strong electric field, thus breaching canonical assumptions of classical electrophysiology. In this context, one structure that is central to signal communication in the brain deserves particular attention, namely, the thin neck of dendritic spines. Here, we refer the reader to a recent review exploring electrodiffusion phenomena pertinent to the electric signal propagation through the spine neck[19]. Detailed theoretical studies have predicted that within such small spaces the local membrane curvature[105] and the surface-volume relationships[106] can also be important in modulating the membrane voltage. Another common scenario involving narrow-space electrodiffusion phenomena arises when an action potential is propagating along an axon that is closely surrounded by neighbouring cellular structures. In this case, the lateral current gives rise to a non-zero electric field inducing lateral electrodiffusion flow of charged molecules within and outside the axonal membrane, thus perturbing the double layer composition[107]. Thus, the microscopic environment of non-myelinated axons could in theory affect spike propagation and local molecular traffic in a mechanistic fashion: future experiments should reveal how exactly this mechanism acts.

Does the theory work with only a few molecules? In some cases, the number of diffusing particles within the volume of interest is so small that the spontaneous fluctuations in their number (owing to their Brownian movement) are comparable to or exceed the average value normally represented by the concentration parameter. For instance, the physiological concentration of 50 nM characterizing free Ca^{2+} in a dendritic spine head or in a nanoscopic astrocyte process corresponds to only a few ions[39,108]. Although in that particular case the small number reflects a dynamic equilibrium between free and bound Ca^{2+} ions (the latter being 100–1000 times more prevalent), Monte Carlo simulations would be required to predict stochastic fluctuations arising from the movements of individual molecules in such cases. It has long been understood that the stochastic processes characteristic for such small volumes (that is, volumes in which only a small number of molecules are present) could play a critical role in molecular dynamics. It has been argued that the thermal noise and the nanoscopic size of the ions affect the amplitude[109] and the variability of the electric current passing through ion channels[110,111]. The finite size of ions inside the sub-membrane double layers can modify the interaction between two neighbouring cell membranes if the inter-membrane clearance is comparable to the thickness of EDLs[112]. The variability of the effective ion concentration influences the sensitivity of membrane receptors, thus setting the limit at which the receptor binding kinetics could be evaluated[113]. In the majority of such cases, there is little choice but to explore such events through Monte Carlo simulations that recapitulate stochastic movements of individual particles.

Membrane proteins and external fields

Lateral electrodiffusion and electro-osmosis of membrane proteins. The phenomenon of lateral electrodiffusion of protein molecules in the plasma membrane in response to extracellularly applied electric field has long been known[15,114]. In cultured embryonic muscle cells, application of a steady extracellular field resulted in the accumulation of ACh receptors towards the cathodal side of the cell and the formation of immobile ACh receptor clusters in the muscle membrane[16]. Interestingly, the removal of cell surface sialic acid with neuraminidase, which reduces the cell surface negative charge, reversed the direction of electrodiffusion[16]. This result is consistent with the idea that the electrodiffusion of membrane proteins is driven not only by '*in situ*' electrophoresis but also by electro-osmosis, in which the flow of cell surface positively charged counter-ions provides the dominate force in dragging negatively charged proteins towards the cathode[115] (as in FIG. 1d; also illustrated in REF. 116). Furthermore, a unipolar pulsed electric field could also induce electrodiffusion towards the cathode[117], suggesting a cumulative effect of the field.

Modulation of cell membrane potential located in external fields. Besides altering the distribution of membrane proteins, extracellular fields also modulate the local membrane potential, with a depolarizing effect on the cathode-facing side of the cell. This membrane potential modulation is particularly pronounced for long processes that are aligned along the direction of the field, given that the voltage drops across the plasma membrane at the two ends of the process are much larger than that across the cell soma. This local membrane potential modulation will in turn affect the extent of activation of

voltage-dependent ion channels. It has been shown that a focal unidirectional pulsed field causes a galvanotropic turning of the axon growth cone towards the current sink generated by a glass microelectrode[118]. This effect on the growth cone could be attributed to the asymmetric local elevation of Ca^{2+} at the growth cone caused by the electric field across the growth cone[119].

Concluding remarks

Numerous theoretical studies and accumulated experimental evidence leave us in little doubt that endogenous neural activities generate strong heterogeneous electric fields within the tissue, particularly in the extracellular space. Such effects become particularly important in restricted spaces, such as small cellular compartments or inside the synaptic cleft. In the latter case, electric fields generated by synaptic currents could directly affect excitatory transmission and its use-dependent changes. To what extent such fields produce direct electrokinetic effects on neural components at a level that could in turn modulate neural functions in a broader context requires further studies. Demonstrating the physiological importance of electrodiffusion phenomena in real-life scenarios remains a critical issue.

The experimental verification of the causality between electrokinetic effects and neural functions is not straightforward, mainly because such effects are often inseparable from other chemical processes associated with electrical activity, but also because direct experimental probing on the nanoscale has severe limitations. For example, demonstrating a direct action of focal electric fields on synaptic receptors would require experimental elimination of the focal fields only, without affecting other chemical processes associated with the synaptic activity, such as Ca^{2+} influx and kinase activation. Nevertheless, the ubiquitous physical presence of endogenous electric fields and the inevitable physical actions of these fields on neuronal components represent a subcellular aspect of the nervous system that deserves more attention and appreciation. By using the movement of electrolytes as a means for communication in the nervous system, the process of evolution could have also taken advantage of various electrokinetic phenomena such as electrodiffusion to serve useful neural functions. With the ever-increasing spatiotemporal resolution of real-time experimental observations in nerve and glial cells, the inclusion of local electrodiffusion phenomena in the interpretation of data is expected to become routine.

1. Triller, A. & Choquet, D. New concepts in synaptic biology derived from single-molecule imaging. *Neuron* **59**, 359–374 (2008).
2. Novak, P. *et al.* Nanoscale-targeted patch-clamp recordings of functional presynaptic ion channels. *Neuron* **79**, 1067–1077 (2013).
3. Hochbaum, D. R. *et al.* All-optical electrophysiology in mammalian neurons using engineered microbial rhodopsins. *Nat. Methods* **11**, 825–833 (2014).
4. Tonnesen, J., Katona, G., Rozsa, B. & Nagerl, U. V. Spine neck plasticity regulates compartmentalization of synapses. *Nat. Neurosci.* **17**, 678–685 (2014).
5. Hodgkin, A. L. & Huxley, A. F. A quantitative description of membrane current and its application to conduction and excitation in nerve. *J. Physiol.* **117**, 500–544 (1952).
6. Buzsaki, G., Anastassiou, C. A. & Koch, C. The origin of extracellular fields and currents—EEG, ECoG, LFP and spikes. *Nat. Rev. Neurosci.* **13**, 407–420 (2012).
7. Pods, J., Schonke, J. & Bastian, P. Electrodiffusion models of neurons and extracellular space using the Poisson-Nernst-Planck equations—numerical simulation of the intra- and extracellular potential for an axon model. *Biophys. J.* **105**, 242–254 (2013).
8. Mori, Y. & Peskin, C. S. A numerical method for cellular electrophysiology based on the electrodiffusion equations with internal boundary conditions at membranes. *Commun. Appl. Math. Computat. Sci.* **4**, 85–134 (2009).
9. Lopreore, C. L. *et al.* Computational modeling of three-dimensional electrodiffusion in biological systems: application to the node of Ranvier. *Biophys. J.* **95**, 2624–2635 (2008).
10. Savtchenko, L. P., Korogod, S. M. & Rusakov, D. A. Electrodiffusion of synaptic receptors: a mechanism to modify synaptic efficacy? *Synapse* **35**, 26–38 (2000).
11. Zhang, L. I. & Poo, M. M. Electrical activity and development of neural circuits. *Nat. Neurosci.* **4**, 1207–1214 (2001).
12. Eccles, J. C. & Jaeger, J. C. The relationship between the mode of operation and the dimensions of the junctional regions at synapses and motor end-organs. *Proc. R. Soc. B* **148**, 38–56 (1958).
This study is a pioneering theoretical work predicting a substantial effect of electric fields on ion currents in small spaces such as the synaptic cleft.
13. Savtchenko, L. P., Antropov, S. N. & Korogod, S. M. Effect of voltage drop within the synaptic cleft on the current and voltage generated at a single synapse. *Biophys. J.* **78**, 1119–1125 (2000).
14. Savtchenko, L. P. & Rusakov, D. A. The optimal height of the synaptic cleft. *Proc. Natl Acad. Sci. USA* **104**, 1823–1828 (2007).
15. Poo, M. M. Insitu electrophoresis of membrane-components. *Annu. Rev. Biophys. Bio* **10**, 245–276 (1981).
16. Orida, N. & Poo, M. M. Electrophoretic movement and localization of acetylcholine receptors in embryonic muscle-cell membrane. *Nature* **275**, 31–35 (1978).
17. Eisenberg, B. Interacting ions in biophysics: real is not ideal. *Biophys. J.* **104**, 1849–1866 (2013).
18. Eisenberg, B. Ionic interactions are everywhere. *Physiol. (Bethesda)* **28**, 28–38 (2013).
19. Holcman, D. & Yuste, R. The new nanophysiology: regulation of ionic flow in neuronal subcompartments. *Nat. Rev. Neurosci.* **16**, 685–692 (2015).
20. Torriero, A. A. J. (ed) *Electrochemistry in Ionic Liquids: Volume 1: Fundamentals* (Springer, 2015).
21. Pods, J. A. Comparison of computational models for the extracellular potential of neurons. *arXiv* http://dx.doi.org/10.3233/JIN-170009 (2015).
22. Luo, Z. X., Xing, Y. Z., Ling, Y. C., Kleinhammes, A. & Wu, Y. Electroneutrality breakdown and specific ion effects in nanoconfined aqueous electrolytes observed by NMR. *Nat. Commun.* **6**, 6358 (2015).
23. DeFelice, L. J. *Electrical Properties of Cells: Patch Clamp for Biologists* (Plenum Press, 1997).
24. Steinberg, J. S. & Mittal, S. *Electrophysiology: the Basics* 2nd edn (Wolters Kluwer Heath, 2017).
25. Macdonald, J. R. A new model for the debye dispersion equations. *Phys. Rev.* **91**, 412–412 (1953).
26. Bagotsky, V. S. (ed.) *Fundamentals of Electrochemistry* 2nd edn (John Wiley & Sons, 2006).
27. Perram, J. W. & Stiles, P. J. On the nature of liquid junction and membrane potentials. *Phys. Chem. Chem. Phys.* **8**, 4200–4213 (2006).
28. Plonsey, R., Henriquez, C. & Trayanova, N. Extracellular (volume conductor) effect on adjoining cardiac muscle electrophysiology. *Med. Biol. Eng. Comput.* **26**, 126–129 (1988).
29. Clark, J. & Plonsey, R. The extracellular potential field of the single active nerve fiber in a volume conductor. *Biophys. J.* **8**, 842–864 (1968).
This study provided an important theoretical introduction to the use of mathematical formalism in calculating extracellular electric fields.
30. Thorne, R. G. & Nicholson, C. *In vivo* diffusion analysis with quantum dots and dextrans predicts the width of brain extracellular space. *Proc. Natl Acad. Sci. USA* **103**, 5567–5572 (2006).
31. Sykova, E. & Nicholson, C. Diffusion in brain extracellular space. *Physiol. Rev.* **88**, 1277–1340 (2008).
32. Hrabetova, S., Hrabe, J. & Nicholson, C. Dead-space microdomains hinder extracellular diffusion in rat neocortex during ischemia. *J. Neurosci.* **23**, 8351–8359 (2003).
33. Kinney, J. P. *et al.* Extracellular sheets and tunnels modulate glutamate diffusion in hippocampal neuropil. *J. Comp. Neurol.* **521**, 448–464 (2013).
34. Zheng, K. *et al.* Nanoscale diffusion in the synaptic cleft and beyond measured with time-resolved fluorescence anisotropy imaging. *Sci. Rep.* **7**, 42022 (2017).
35. Rusakov, D. A. & Kullmann, D. M. Geometric and viscous components of the tortuosity of the extracellular space in the brain. *Proc. Natl Acad. Sci. USA* **95**, 8975–8980 (1998).
36. Hrabetova, S., Masri, D., Tao, L., Xiao, F. & Nicholson, C. Calcium diffusion enhanced after cleavage of negatively charged components of brain extracellular matrix by chondroitinase ABC. *J. Physiol.* **587**, 4029–4049 (2009).
37. Miranda, P. C., Hallett, M. & Basser, P. J. The electric field induced in the brain by magnetic stimulation: a 3D finite-element analysis of the effect of tissue heterogeneity and anisotropy. *IEEE Trans. Biomed. Eng.* **50**, 1074–1085 (2003).
38. Bazhenov, M., Lonjers, P., Skorheim, S., Bedard, C. & Dstexhe, A. Non-homogeneous extracellular resistivity affects the current-source density profiles of up-down state oscillations. *Philos. Trans. A Math. Phys. Eng. Sci.* **369**, 3802–3819 (2011).
39. Rusakov, D. A. Disentangling calcium-driven astrocyte physiology. *Nat. Rev. Neurosci.* **16**, 226–233 (2015).
40. Gleixner, R. & Fromherz, P. The extracellular electrical resistivity in cell adhesion. *Biophys. J.* **90**, 2600–2611 (2006).
41. Rudy, Y. & Plonsey, R. Volume conductor and geometrical effects on body-surface and epicardial potentials.1. *Theory. Phys. Med. Biol.* **25**, 978–978 (1980).
42. Hallez, H. *et al.* Review on solving the forward problem in EEG source analysis. *J. Neuroeng. Rehabil.* **4**, 46 (2007).
43. McLaughlin, S. The electrostatic properties of membranes. *Annu. Rev. Biophys. Biophys. Chem.* **18**, 113–136 (1989).

44. Greathouse, J. A., Feller, S. E. & Mcquarrie, D. A. The modified Gouy-Chapman theory - comparisons between electrical double-layer models of clay swelling. *Langmuir* **10**, 2125–2130 (1994).
45. Zheng, K., Scimemi, A. & Rusakov, D. A. Receptor actions of synaptically released glutamate: the role of transporters on the scale from nanometers to microns. *Biophys. J.* **95**, 4584–4596 (2008).
46. Nadler, B., Naeh, T. & Schuss, Z. Connecting a discrete ionic simulation to a continuum. *SIAM J. Appl. Math.* **63**, 850–873 (2003).
47. Sylantyev, S., Savtchenko, L. P., Ermolyuk, Y., Michaluk, P. & Rusakov, D. A. Spike-driven glutamate electrodiffusion triggers synaptic potentiation via a Homer-dependent mGluR-NMDAR link. *Neuron* **77**, 528–541 (2013).
48. Guerrier, C. & Holcman, D. Hybrid Markov-mass action law model for cell activation by rare binding events: application to calcium induced vesicular release at neuronal synapses. *Sci. Rep.* **6**, 35506 (2016).
49. Marhl, M., Brumen, M., Glaser, R. & Heinrich, R. Diffusion layer caused by local ionic transmembrane fluxes. *Pflugers Arch.* **431**, R259–R260 (1996).
50. McLaughlin, S. G., Szabo, G. & Eisenman, G. Divalent ions and the surface potential of charged phospholipid membranes. *J. Gen. Physiol.* **58**, 667–687 (1971).
51. Ward, K. R., Dickinson, E. J. F. & Compton, R. G. How far do membrane potentials extend in space beyond the membrane itself? *Int. J. Electrochem. Sci.* **5**, 1527–1534 (2010).
52. Stuart, G., Schiller, J. & Sakmann, B. Action potential initiation and propagation in rat neocortical pyramidal neurons. *J. Physiol.-Lond.* **505**, 617–632 (1997).
53. Bezanilla, F. The voltage sensor in voltage-dependent ion channels. *Physiol. Rev.* **80**, 555–592 (2000).
54. Catterall, W. A. Ion channel voltage sensors: structure, function, and pathophysiology. *Neuron* **67**, 915–928 (2010).
55. Neher, E. Correction for liquid junction potentials in patch clamp experiments. *Method Enzymol.* **207**, 123–131 (1992).
56. von J. J. Lingane. *Electroanalytical Chemistry* (Interscience Publishers, 1958).
57. Dickinson, E. J., Freitag, L. & Compton, R. G. Dynamic theory of liquid junction potentials. *J. Phys. Chem. B* **114**, 187–197 (2010).
58. Barton, P. G. The influence of surface charge density of phosphatides on the binding of some cations. *J. Biol. Chem.* **243**, 3884–3890 (1968).
59. Gurtovenko, A. A. & Vattulainen, I. Membrane potential and electrostatics of phospholipid bilayers with asymmetric transmembrane distribution of anionic lipids. *J. Phys. Chem. B* **112**, 4629–4634 (2008).
60. van Meer, G., Voelker, D. R. & Feigenson, G. W. Membrane lipids: where they are and how they behave. *Nat. Rev. Mol. Cell Biol.* **9**, 112–124 (2008).
61. Isaev, D. *et al.* Surface charge impact in low-magnesium model of seizure in rat hippocampus. *J. Neurophysiol.* **107**, 417–423 (2012).
62. Rusakov, D. A. & Fine, A. Extracellular Ca^{2+} depletion contributes to fast activity-dependent modulation of synaptic transmission in the brain. *Neuron* **37**, 287–297 (2003).
63. Annunziato, L., Pignataro, G. & Di Renzo, G. F. Pharmacology of brain Na^{+}/Ca^{2+} exchanger: from molecular biology to therapeutic perspectives. *Pharmacol. Rev.* **56**, 633–654 (2004).
64. Hahin, R. & Campbell, D. T. Simple shifts in the voltage dependence of sodium channel gating caused by divalent cations. *J. Gen. Physiol.* **82**, 785–805 (1983).
65. Hille, B., Woodhull, A. M. & Shapiro, B. I. Negative surface charge near sodium channels of nerve: divalent ions, monovalent ions, and pH. *Phil. Trans. R. Soc. Lond. B* **270**, 301–318 (1975).
66. Isaev, D. *et al.* Role of extracellular sialic acid in regulation of neuronal and network excitability in the rat hippocampus. *J. Neurosci.* **27**, 11587–11594 (2007).
67. Ednie, A. R. & Bennett, E. S. Modulation of voltage-gated ion channels by sialylation. *Compr. Physiol.* **2**, 1269–1301 (2012).
68. Michaluk, P. *et al.* Matrix metalloproteinase-9 controls NMDA receptor surface diffusion through integrin β1 signaling. *J. Neurosci.* **29**, 6007–6012 (2009).
69. Kochlamazashvili, G. *et al.* The extracellular matrix molecule hyaluronic acid regulates hippocampal synaptic plasticity by modulating postsynaptic L-type Ca^{2+} channels. *Neuron* **67**, 116–128 (2010).
70. Dityatev, A., Schachner, M. & Sonderegger, P. The dual role of the extracellular matrix in synaptic plasticity and homeostasis. *Nat. Rev. Neurosci.* **11**, 735–746 (2010).
71. Young, S. H. & Poo, M. M. Topographical rearrangement of acetylcholine receptors alters channel kinetics. *Nature* **304**, 161–163 (1983).
72. Qian, N. & Sejnowski, T. J. An electro-diffusion model for computing membrane-potentials and ionic concentrations in branching dendrites, spines and axons. *Biol. Cybern.* **62**, 1–15 (1989).
This paper provides a clear and detailed outline of the mathematical formalism of electrodiffusion pertinent to small spaces in the microenvironment of dendrites and synapses.
73. Langlands, T. A., Henry, B. I. & Wearne, S. L. Fractional cable equation models for anomalous electrodiffusion in nerve cells: infinite domain solutions. *J. Math. Biol.* **59**, 761–808 (2009).
74. Henry, B. I., Langlands, T. A. & Wearne, S. L. Fractional cable models for spiny neuronal dendrites. *Phys. Rev. Lett.* **100**, 128103 (2008).
75. Halnes, G., Ostby, I., Pettersen, K. H., Omholt, S. W. & Einevoll, G. T. Electrodiffusive model for astrocytic and neuronal ion concentration dynamics. *PLoS Comput. Biol.* **9**, e1003386 (2013).
76. Halnes, G., Ostby, I., Pettersen, K. H., Omholt, S. W. & Einevoll, G. T. in *Advances in Cognitive Neurodynamics (IV)* (ed. Liljenström, H.) 353–360 (2015).
77. Gianazza, E. & Righetti, P. G. Size and charge-distribution of macromolecules in living systems. *J. Chromatogr.* **193**, 1–8 (1980).
78. Lodish, H. F. *Molecular cell biology* 4th edn (W. H. Freeman, 2000).
79. Glykys, J. *et al.* Local impermeant anions establish the neuronal chloride concentration. *Science* **343**, 670–675 (2014).
80. Voipio, J. *et al.* Comment on "Local impermeant anions establish the neuronal chloride concentration". *Science* **345**, 1130 (2014).
81. Kaila, K., Price, T. J., Payne, J. A., Puskarjov, M. & Voipio, J. Cation-chloride cotransporters in neuronal development, plasticity and disease. *Nat. Rev. Neurosci.* **15**, 637–654 (2014).
82. Doyon, N., Vinay, L., Prescott, S. A. & De Koninck, Y. Chloride regulation: a dynamic equilibrium crucial for synaptic inhibition. *Neuron* **89**, 1157–1172 (2016).
83. Luby-Phelps, K. The physical chemistry of cytoplasm and its influence on cell function: an update. *Mol. Biol. Cell* **24**, 2593–2596 (2013).
84. Luby-Phelps, K. Cytoarchitecture and physical properties of cytoplasm: volume, viscosity, diffusion, intracellular surface area. *Int. Rev. Cytol.* **192**, 189–221 (2000).
85. Leterrier, J. F. Water and the cytoskeleton. *Cell. Mol. Biol. (Noisy-le-Grand)* **47**, 901–923 (2001).
86. Fels, J., Orlov, S. N. & Grygorczyk, R. The hydrogel nature of mammalian cytoplasm contributes to osmosensing and extracellular pH sensing. *Biophys. J.* **96**, 4276–4285 (2009).
87. Janmey, P. A., Slochower, D. R., Wang, Y. H., Wen, Q. & Cebers, A. Polyelectrolyte properties of filamentous biopolymers and their consequences in biological fluids. *Soft Matter* **10**, 1439–1449 (2014).
88. Verkman, A. S. Solute and macromolecule diffusion in cellular aqueous compartments. *Trends Biochem. Sci.* **27**, 27–33 (2002).
89. Tuszynski, J. A., Portet, S., Dixon, J. M., Luxford, C. & Cantiello, H. F. Ionic wave propagation along actin filaments. *Biophys. J.* **86**, 1890–1903 (2004).
90. Kekenes-Huskey, P. M., Scott, C. E. & Atalay, S. Quantifying the influence of the crowded cytoplasm on small molecule diffusion. *J. Phys. Chem. B* **120**, 8696–8770 (2016).
91. Eccles, J. C. *The Physiology of Synapses* (Springer-Verlag, 1964).
92. Poo, M. M. & Young, S. H. Diffusional and electrokinetic redistribution at the synapse - a physicochemical basis of synaptic competition. *J. Neurobiol.* **21**, 157–168 (1990).
93. Sylantyev, S. *et al.* Electric fields due to synaptic currents sharpen excitatory transmission. *Science* **319**, 1845–1849 (2008).
This study provided the first experimental demonstration of electrodiffusion phenomena affecting glutamatergic transmission in the synaptic cleft.
94. Xie, Z. P. & Poo, M. M. Initial events in the formation of neuromuscular synapse - rapid induction of acetylcholine-release from embryonic neuron. *Proc. Natl Acad. Sci. USA* **83**, 7069–7073 (1986).
95. Groc, L. *et al.* Differential activity-dependent regulation of the lateral mobilities of AMPA and NMDA receptors. *Nat. Neurosci.* **7**, 695–696 (2004).
96. Ashby, M. C., Maier, S. R., Nishimune, A. & Henley, J. M. Lateral diffusion drives constitutive exchange of AMPA receptors at dendritic spines and is regulated by spine morphology. *J. Neurosci.* **26**, 7046–7055 (2006).
97. Anantharam, V. *et al.* Combinatorial RNA splicing alters the surface-charge on the nmda receptor. *Febs Lett.* **305**, 27–30 (1992).
98. Choquet, D. & Triller, A. The role of receptor diffusion in the organization of the postsynaptic membrane. *Nat. Rev. Neurosci.* **4**, 251–265 (2003).
99. Seeliger, C. & Le Novere, N. Enabling surface dependent diffusion in spatial simulations using Smoldyn. *BMC Res. Notes* **8**, 752 (2015).
100. Constals, A. *et al.* Glutamate-induced AMPA receptor desensitization increases their mobility and modulates short-term plasticity through unbinding from Stargazin. *Neuron* **85**, 787–803 (2015).
101. Czondor, K. *et al.* Unified quantitative model of AMPA receptor trafficking at synapses. *Proc. Natl Acad. Sci. USA* **109**, 3522–3527 (2012).
102. Bliss, T. & Lomo, T. Long-lasting potentiation of synaptic transmission in the dentate area of the anaesthetized rabbit following stimulation of the perforant path. *J. Physiol.* **232**, 331–356 (1973).
103. Ehlers, M. D., Heine, M., Groc, L., Lee, M. C. & Choquet, D. Diffusional trapping of GluR1 AMPA receptors by input-specific synaptic activity. *Neuron* **54**, 447–460 (2007).
104. Meier, J., Vannier, C., Serge, A., Triller, A. & Choquet, D. Fast and reversible trapping of surface glycine receptors by gephyrin. *Nat. Neurosci.* **4**, 253–260 (2001).
105. Cartailler, J., Schuss, Z. & Holcman, D. Analysis of the Poisson-Nernst-Planck equation in a ball for modeling the Voltage-Current relation in neurobiological microdomains. *Phys. D-Nonlinear Phenomena* **339**, 39–48 (2017).
106. Cartailler, J., Schuss, Z. & Holcman, D. Electrostatics of non-neutral biological microdomains. *arXiv* 1612.07941 (2016).
This paper provides the most complete mathematical description to date of electrolyte electrodynamics in small cellular compartments.
107. Shilov, V., Barany, S., Grosse, C. & Shramko, O. Field-induced disturbance of the double layer electro-neutrality and non-linear electrophoresis. *Adv. Colloid Interface Sci.* **104**, 159–173 (2003).
108. Grienberger, C. & Konnerth, A. Imaging calcium in neurons. *Neuron* **73**, 862–885 (2012).
109. Bauer, M., Godec, A. & Metzler, R. Diffusion of finite-size particles in two-dimensional channels with random wall configurations. *Phys. Chem. Chem. Phys.* **16**, 6118–6128 (2014).
110. Zitserman, V. Y., Berezhkovskii, A. M., Pustovoit, M. A. & Bezrukov, S. M. Relaxation and fluctuations of the number of particles in a membrane channel at arbitrary particle-channel interaction. *J. Chem. Phys.* **129**, 095101 (2008).
111. Mak, D. O. & Webb, W. W. Conductivity noise in transmembrane ion channels due to ion concentration fluctuations via diffusion. *Biophys. J.* **72**, 1153–1164 (1997).
112. Das, S. Electric-double-layer potential distribution in multiple-layer immiscible electrolytes: effect of finite ion sizes. *Phys. Rev. E Stat. Nonlin. Soft Matter Phys.* **85**, 012502 (2012).
This paper presents a theoretical investigation that reveals how the size of ions can affect the electric field profile near charged cell membranes.

113. Bialek, W. & Setayeshgar, S. Physical limits to biochemical signaling. *Proc. Natl Acad. Sci. USA* **102**, 10040–10045 (2005).
114. Poo, M. & Robinson, K. R. Electrophoresis of concanavalin A receptors along embryonic muscle cell membrane. *Nature* **265**, 602–605 (1977).
115. Mclaughlin, S. & Poo, M. M. The role of electroosmosis in the electric-field-induced movement of charged macromolecules on the surfaces of cells. *Biophys. J.* **34**, 85–93 (1981).
This work is the first study to show experimentally and to explain theoretically the effect of electro-osmosis on the lateral redistribution of membrane components.
116. Rusakov, D. A., Savtchenko, L. P., Zheng, K. & Henley, J. M. Shaping the synaptic signal: molecular mobility inside and outside the cleft. *Trends Neurosci.* **34**, 359–369 (2011).
117. Linliu, S., Adey, W. R. & Poo, M. M. Migration of cell-surface concanavalin a receptors in pulsed electric-fields. *Biophys. J.* **45**, 1211–1217 (1984).
118. Patel, N. B. & Poo, M. M. Perturbation of the direction of neurite growth by pulsed and focal electric-fields. *J. Neurosci.* **4**, 2939–2947 (1984).
119. Henley, J. & Poo, M. Guiding neuronal growth cones using Ca^{2+} signals. *Trends Cell Biol.* **14**, 320–330 (2004).
120. Dufreche, J. F., Jardat, M., Turq, P. & Bagchi, B. Electrostatic relaxation and hydrodynamic interactions for self-diffusion of ions in electrolyte solutions. *J. Phys. Chem. B* **112**, 10264–10271 (2008).
121. Kobelev, V., Kolomeisky, A. B. & Panagiotopoulos, A. Z. Thermodynamics of electrolytes on anisotropic lattices. *Phys. Rev. E Stat. Nonlin. Soft Matter Phys.* **68**, 066110 (2003).

Acknowledgements.
This work was supported by the Wellcome Trust Principal Fellowship, a European Research Council Advanced Grant (323113-NETSIGNAL), a Russian Science Foundation grant (15-14-30000, FIG. 1 data) and FP7 ITN (606950 EXTRABRAIN). (101896).

Author contributions
The authors all researched data for the article, made substantial contributions to discussions of the content, wrote the article and reviewed and/or edited the manuscript before submission.

Competing interests statement
The authors declare no competing interests.

Publisher's note
Springer Nature remains neutral with regard to jurisdictional claims in published maps and institutional affiliations.